

Broadband CPW-Fed Circularly Polarized Square Slot Antenna for Universal UHF RFID Handheld Reader

Rui Ma and Quanyuan Feng

Department of Information Science and Technology
Southwest Jiaotong University, Chengdu, 611756, China
marui971213@163.com, fengquanyuan@163.com

Abstract — This paper presents a new coplanar waveguide (CPW)-fed circularly polarized square slot antenna (CPSSA). The proposed antenna uses an inverted Z-shaped feedline protruded from the signal line of the feeding CPW. Circularly polarized (CP) radiation can be achieved by adequately inserting the arc-shaped grounded strip into the upper right corner of the square slot. The widened vertical tuning stub on the L-shaped grounded strip can improve impedance matching and axial ratio (AR) performance. The measured results indicate that the 10 dB impedance bandwidth is 620 MHz (652-1272 MHz), and the 3 dB axial ratio bandwidth is 320 MHz (840-1160 MHz), which has a broadband characteristic. In the range of the universal UHF RFID band, the measured peak gain is about 4.4 dBi. The proposed CPSSA uses low-cost FR4 material as the dielectric substrate. The overall size of the antenna is $119 \times 119 \times 0.5 \text{ mm}^3$. The proposed antenna has a simple structure, easy processing, good performance, wide operating bandwidth, and dual circular polarization characteristic. It can be applied to the universal UHF RFID handheld reader environment.

Index Terms — Circularly polarized, CPW-fed, handheld reader, UHF RFID.

I. INTRODUCTION

Radio-frequency identification (RFID) is a wireless communication technology that uses electromagnetic waves to identify and track objects [1]. RFID technology has the advantages of high accuracy, long reading distance, fast reading speed, strong environmental adaptability, and non-contact. It is widely applied to product tracking, goods flow system, traffic management, medical-care systems, automobile safety, etc. A typical RFID system generally consists of an electronic tag and a reader device. The reader device uses the reader antenna to send radio frequency signals to the tag and receive the tag information [2]. Since the RFID tag is linearly polarized (LP), and the placement orientation of the tag is arbitrary, CP operation can reduce the loss caused by the polarization mismatch and the multipath

effect between the tag antenna and the reader antenna, and improve communication reliability. In the practical RFID applications, the circularly polarized antennas [3-5] are usually required. RFID system can be divided into low frequency (LF), high frequency (HF), ultra-high frequency (UHF), and microwave (MW) frequency bands [6]. UHF RFID has the characteristics of long readable distance, large information storage capacity, and high data transfer rate. Therefore, it is of great significance to study CP reader antennas that cover the universal UHF RFID band. The frequency bands authorized for UHF RFID applications are different in different countries and regions, like 840-845 MHz and 920-925 MHz in China, 908.5-914 MHz in South Korea, 952-955 MHz in Japan, 865-867 MHz in India, 902-928 MHz in America, 866-869 MHz and 920-925 MHz in Singapore, and 920-926 MHz in Australia [7]. The frequency range of the universal UHF RFID is from 840 to 960 MHz.

Numerous circularly polarized reader antennas have been proposed for RFID systems. A novel circularly polarized annular-ring microstrip antenna is presented [8]. The CP operation is realized by an equal-split divided power divider with a phase difference of 90° . In [9], The CP antenna operating within the universal UHF RFID frequency range adopts the technology of loading a corner-truncated square patch to achieve good impedance matching and circular polarization characteristics. In [10-11], the main patch is fed by four adjacent probes sequentially connected to the suspended feeding strip to achieve CP radiation. A circularly polarized stack Yagi antenna for RFID reader applications is proposed [12]. The circular polarization performance is achieved by straight cutting on the two edges of the main patch, the parasitic patch, and the director patch. The above-mentioned CP antennas have wide operating bandwidth and high gain, but they have the disadvantages such as complex structure, complicated processing, large antenna dimension, and poor portability. The printed slot antennas [13-16] have the characteristics of small size, low cost, easy fabrication, and wide coverage bandwidth. Many articles have studied slot antennas. A circularly

proposed antenna are described by five prototypes from Ant. I to Ant. V. Figures 3 (a) and (b) present the simulated results of the frequency response of the reflection coefficient S_{11} and the axial ratio for Ant. I to Ant. V. The wide slot antenna has wide bandwidth characteristic, so the ground plane of Ant. I is designed as a wide square slot structure with an L-shaped feedline. From the simulated results of S_{11} and AR, it is found that the 10 dB impedance bandwidth of Ant. I does not cover the entire UHF RFID band, and linearly polarized waves are radiated. The 10 dB impedance bandwidth is from 0.69 GHz to 0.75 GHz and from 0.93 GHz to 1.09 GHz, and the axial ratio in the frequency band of 0.7-1.3 GHz is much greater than 3 dB, and CP radiation is not realized. In Ant. II, an L-shaped grounded strip is added to the lower-left corner of the square slot to enhance the capacitive coupling between the ground plane and the feed structure, thereby broadening the bandwidth of the antenna. The impedance matching characteristic of Ant. II becomes worse, but the axial ratio is closer to 3 dB, and the CP radiation is still not realized. Ant. III has a vertical strip with a length of L_5 in the vertical direction embedded in the feed structure. As shown by the simulated results of Ant. III, the impedance matching characteristic is improved, and the 10 dB impedance bandwidth is from 0.65 GHz to 0.72 GHz and from 0.87 GHz to 1.08 GHz. The axial ratio in the entire UHF RFID band is about 14 dB. In Ant. IV, an arc-shaped grounded strip is inserted into the upper right corner of the square slot, which interferes with the current distribution in the square slot. In the universal UHF RFID band, the axial ratio is less than 3 dB, which realizes CP radiation and obtains the wide impedance bandwidth and axial ratio bandwidth. The 10 dB impedance bandwidth is from 0.64 GHz to 0.73 GHz and from 0.74 GHz to 1.05 GHz, and the 3 dB axial ratio bandwidth is from 0.83 GHz to 1.16 GHz, realizing broadband and circular polarization characteristics. The S_{11} of Ant. IV achieves a minimum value of -17.68 dB at the resonant frequency of 0.86 GHz. In order to further optimize the performance of the antenna, by widening the vertical tuning stub of the grounded L-shaped strip embedded in the square slot to obtain Ant. V, good impedance matching characteristic can be achieved, and the impedance matching bandwidth and the axial ratio bandwidth are further broadened. The simulated results show that in the entire UHF RFID band, the S_{11} of Ant. V at the resonance frequency of 0.90 GHz achieves the minimum value of -23.68 dB. The 10 dB impedance bandwidth is from 0.64 GHz to 1.27 GHz, and the 3 dB axial ratio bandwidth is from 0.83 GHz to 1.19 GHz. Finally, the proposed CPSSA has a very wide bandwidth coverage, which meets the requirements of covering the universal UHF RFID frequency range.

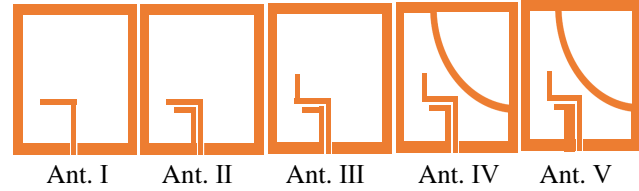


Fig. 2. Five prototypes of the proposed antenna.

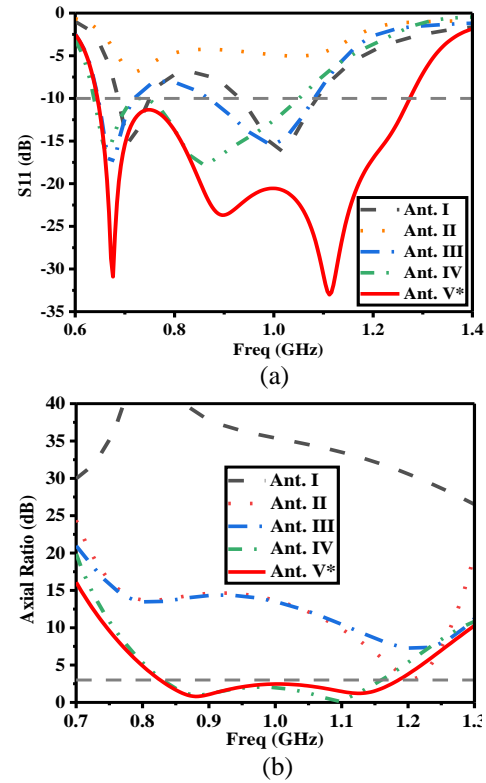


Fig. 3. Simulated results for antennas I-V: (a) reflection coefficient and (b) axial ratio.

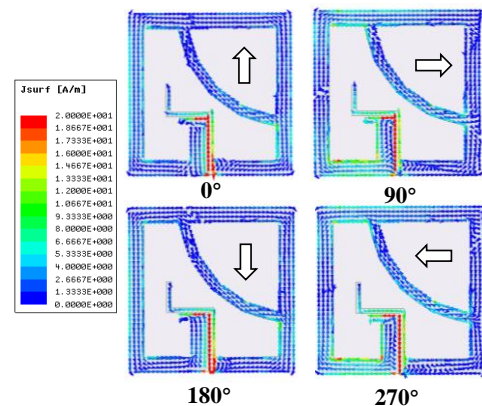


Fig. 4. Surface current distributions of the proposed CPSSA at 900 MHz in 0° , 90° , 180° , and 270° .

In order to explain the mechanism of CP radiation, the surface current distribution of the proposed CPSSA at 900 MHz with four phase angles of 0° , 90° , 180° , and 270° are illustrated in Fig. 4. As shown in the figure, it is observed the surface current distribution with the phase angle of 180° and 270° are opposite to the phase angle of 0° and 90° , respectively. The surface current rotates in a clockwise direction as the phase angle increases by 90° . Therefore, the proposed antenna excites left-handed circular polarization (LHCP) radiation in the $+Z$ direction and right-handed circular polarization (RHCP) radiation in the $-Z$ direction, which has dual circular polarization characteristic. The RHCP radiation can be excited in the $+Z$ direction by simultaneously inverting the directions of the inverted Z-shaped feedline, the arc-shaped grounded strip, and the L-shaped grounded strip with respect to the Y -axis.

III. PARAMETERS STUDIES

Parameter studies are to obtain the optimal impedance matching and CP performance. In this section, the key parameters of the proposed antenna are simulated and optimized using Ansoft HFSS 18.0. The simulated results illustrate the influence of key parameters such as the outer radius of the arc-shaped grounded strip (R_1), the length of the vertical strip of the inverted Z-shaped feedline (L_5), and the width of the vertical tuning stub of the L-shaped grounded strip (W_2) on the reflection coefficient S_{11} and AR bandwidth. When optimizing the parameters, make sure that one parameter is varied, while the other parameters are fixed.

A. Effects of the arc-shaped grounded strip

Good CP performance can be obtained by adequately adjusting the outer radius of the arc-shaped grounded strip (R_1). Figure 5 exhibits the effects of R_1 on the S_{11} and axial ratio. It can be seen from Fig. 5 (a) that different values of R_1 have little effect on the starting frequencies and low-frequency resonance frequencies. As R_1 increases, the high-frequency resonance frequency shifts to lower frequencies, and the stop frequency shifts to higher frequencies. Therefore, the thicker the arc-shaped grounded strip, the wider the 10 dB impedance matching bandwidth. When R_1 is 85.5 mm, the 10 dB impedance bandwidth is the widest, which is from 0.64 GHz to 1.27 GHz. Figure 5 (b) shows the effect of R_1 on the axial ratio. It is observed that as the value of R_1 increases, the low-frequency resonance frequency shifts to higher frequencies, whereas the high-frequency resonance frequency shifts to lower frequencies. Except for $R_1=85.5$ mm, as the thickness of the arc-shaped grounded strip is thicker, the axial ratio bandwidth is wider. When R_1 is 79.5 mm, the 3 dB axial ratio bandwidth is from 0.81 GHz to 0.94 GHz, which can't totally cover the specification of the universal UHF RFID band. When R_1 is 83.5 mm, the 3 dB AR bandwidth is

the widest, ranging from 0.83 GHz to 1.19 GHz, which meets the required bandwidth requirement. The axial ratio at the low-frequency resonance frequency of 0.88 GHz is 0.79 dB. It is worth noting that by adjusting the value of R_1 , that is, adjusting the thickness of the arc-shaped grounded strip, the AR bandwidth can be reconfigured to cover the required UHF RFID frequency range.

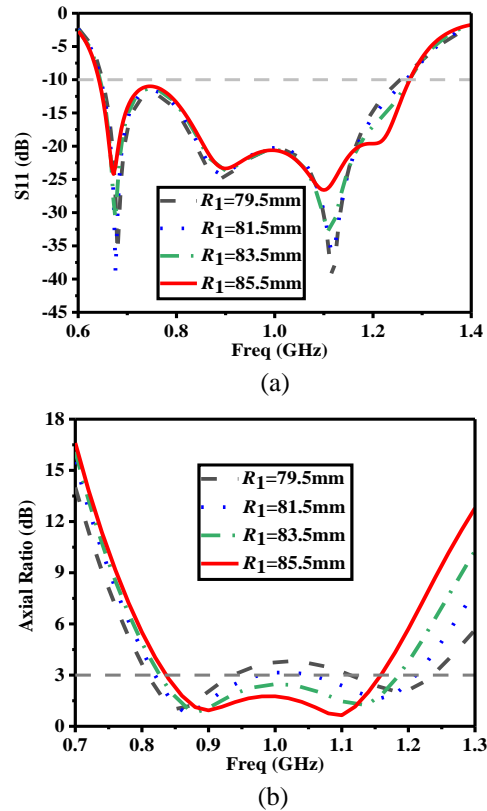


Fig. 5. Simulated results for the proposed broadband CPSSA with different outer radii (R_1) of the arc-shaped grounded strip: (a) S_{11} and (b) axial ratio.

B. Effects of the inverted Z-shaped feedline

Figure 6 shows the influence of the length of the vertical strip of the inverted Z-shaped feedline (L_5) on the antenna performance. Figure 6 (a) illustrates the effect of L_5 on impedance matching characteristic. It is found that when L_5 is increased, both the start frequency and the low-frequency resonance frequency slightly shift to lower frequencies, the high-frequency resonance frequency shifts to higher frequencies. When L_5 is 18.5 mm, the 10 dB impedance bandwidth is the narrowest. When L_5 takes other values, the impedance bandwidth is not much different, but when $L_5=22.5$ mm, the impedance matching characteristic is the best in the universal UHF RFID frequency range. The effect of L_5 on the AR performance is shown in Fig. 6 (b). Different

values of L_5 have a very slight influence on the resonance frequency and the 3 dB axial ratio bandwidth. The parameter L_5 has almost no effect on the axial ratio, which shows that L_5 has strong manufacture tolerance for the proposed broadband CPSSA. When L_5 takes the value of 22.5 mm, the proposed antenna has good impedance matching performance and the 3 dB axial ratio bandwidth is the widest, so the optimal value of L_5 is 22.5 mm.

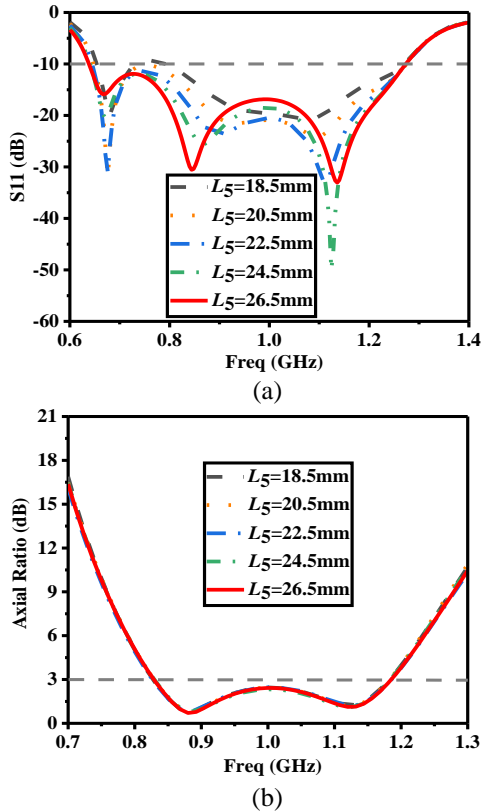


Fig. 6. Simulated results for the proposed broadband CPSSA with different vertical lengths (L_5) of the inverted Z-shaped feedline: (a) S_{11} and (b) axial ratio.

C. Effects of the L-shaped grounded strip

The simulated results of S_{11} and AR versus frequency for the different width of the vertical tuning stub of the L-shaped grounded strip (W_2) is demonstrated in Fig. 7. The simulated S_{11} shows that different values of parameter W_2 have a greater effect on the high-frequency resonance frequency. As the value of W_2 increases, the high-frequency resonance frequency shifts to higher frequencies, and the impedance bandwidth becomes wider. When W_2 is 14 mm, the 10 dB impedance bandwidth is the widest, ranging from 0.64 GHz to 1.29 GHz. Whereas, in the frequency range of 840-960 MHz, the impedance matching characteristic when $W_2 = 12$ mm is better than that when $W_2 = 14$ mm. From the influence of W_2 on the axial ratio characteristic, it is found that the

smaller the value of W_2 , the wider the axial ratio bandwidth, and the different values of W_2 have little influence on the resonance frequency.

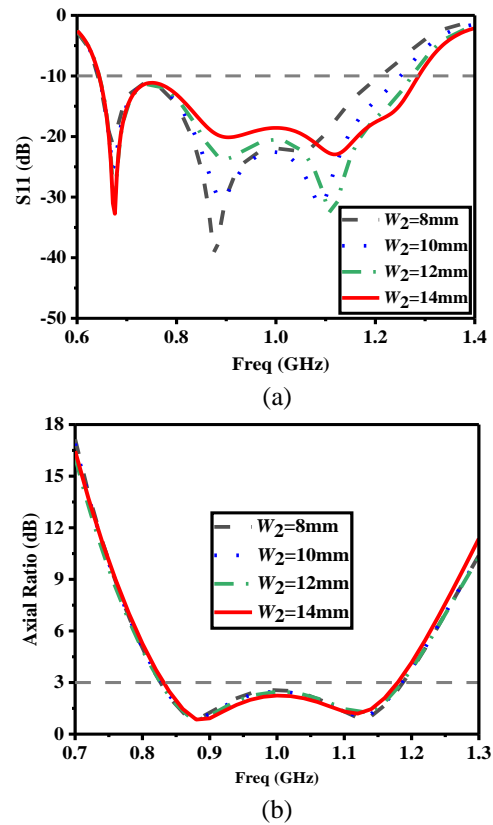


Fig. 7. Simulated results for the proposed broadband CPSSA with different vertical lengths (W_2) of the L-shaped grounded strip: (a) S_{11} and (b) axial ratio.

IV. RESULTS AND DISCUSSION

Figure 8 shows the manufactured prototype and far-field measurement photograph of the proposed CPSSA with the optimum values. The reflection coefficient S_{11} is measured by an Agilent E5071C vector network analyzer. The simulated and experimental reflection coefficient S_{11} of the proposed antenna are exhibited in Fig. 9. The measured 10 dB impedance bandwidth is 64.4% (652-1272 MHz), which agrees well with the simulated 10 dB impedance bandwidth (640-1270 MHz). The minimum values of the simulated and measured results of S_{11} are -33.02 dB and -40.30 dB, respectively. The curve trend of the impedance matching of simulation and measurement is roughly similar. The far-field performances of the proposed antenna, such as axial ratio, gain, radiation efficiency and 2D radiation pattern, are all tested in an anechoic chamber using the SATIMO measurement system. Figure 10 illustrates the comparison of the simulated and measured results of AR. The measured 3 dB AR bandwidth is 32.0% (840-1160 MHz),

which is narrower than the simulated results (830-1190 MHz). The simulated and measured 3 dB AR bandwidths are wide, covering the entire UHF RFID band. The simulated and measured results of peak gain and radiation efficiency are shown in Fig. 11. In the UHF RFID frequency range (840-960 MHz), the measured peak gain fluctuates within 3.4-4.6 dBi. The measured maximum peak gain is 4.6 dBi at 960 MHz and the measured radiation efficiency is about 90%. The slight difference between the simulated and measured results of peak gain and radiation efficiency is mainly attributed to the manufacturing tolerances. Figure 12 shows the simulated and measured LHCP/RHCP radiation patterns for the x-z and y-z planes at the center frequency of 900 MHz in the universal UHF RFID band. The measured results of the radiation patterns in both x-z and y-z planes demonstrate that the proposed antenna has good bidirectional characteristic.

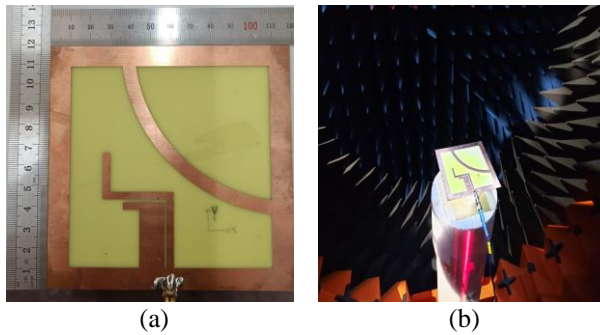


Fig. 8. Photographs of the proposed antenna: (a) manufactured prototype, and (b) far-field measurement.

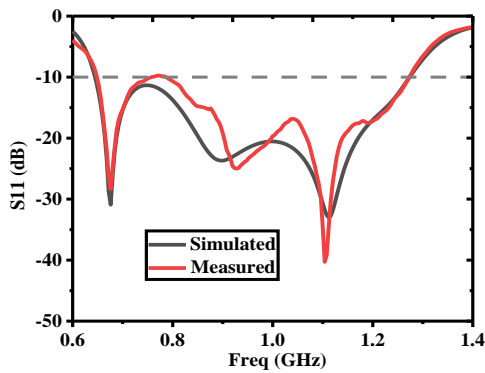


Fig. 9. Simulated and measured reflection coefficient of the proposed broadband CPSSA.

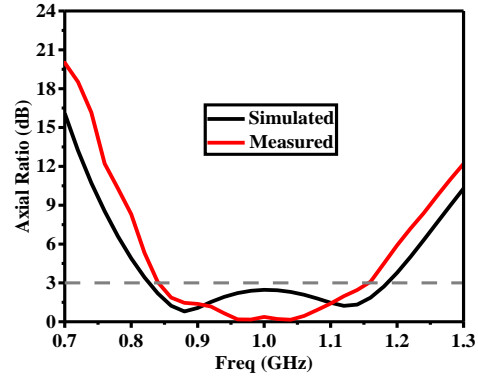


Fig. 10. Simulated and measured axial ratio of the proposed broadband CPSSA.

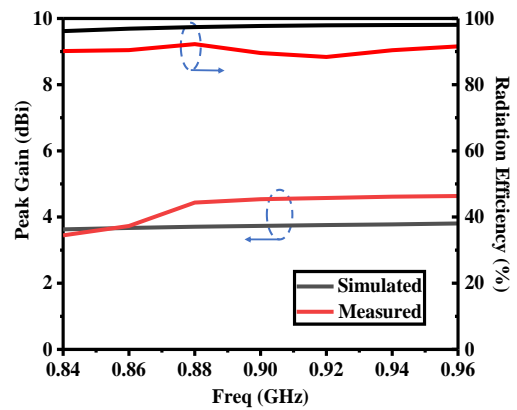


Fig. 11. Simulated and measured peak gain and radiation efficiency of the proposed antenna.

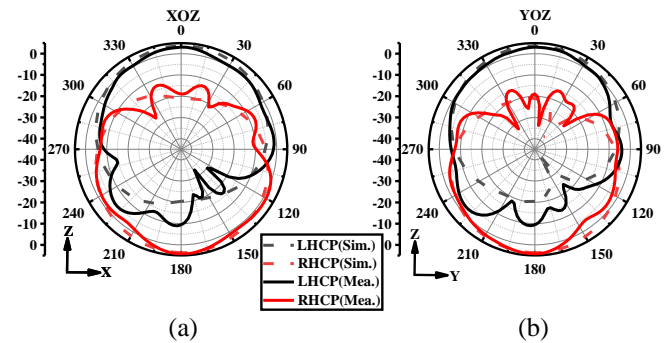


Fig. 12. Simulated and measured LHCP and RHCP radiation patterns of the proposed antenna at 900 MHz: (a) x-z and (b) y-z planes.

Table 1: Comparison of the proposed antenna with other CP antennas in references

Ref.	Impedance Bandwidth (MHz, %)	3 dB AR Bandwidth (MHz, %)	Dimensions $L \times W \times H$ (mm ³)
[5]	835–975, 16.4%	870-940, 7.7%	124× 117 × 33.2
[8]	870-967, 10.6%	893-948, 6%	220 × 220 × 10
[10]	768-962, 22.4%	816-957, 15.9%	250 × 250 × 35
[18]	800-1056, 28.5%	900-936, 4%	90 × 105 × 1.6
[21]	815–925, 12.6%	835-870, 4.3%	83 × 83 × 1.6
Proposed	652-1272, 64%	840-1160, 32.0%	119 × 119 × 0.5

Table 1 exhibits the comparison between the proposed broadband CPSSA and the other CP antennas for UHF RFID reader. As shown in Table 1, the proposed antenna covers the universal UHF RFID band and has the merits of wide operating bandwidth and small volume, which is more suitable for universal UHF RFID handheld reader applications than the other CP antennas in the references. Compared with the CP antennas in [18, 21], the antennas in the literature [5, 8, 10] have the wider S_{11} and AR bandwidth, but the corresponding operating bandwidths do not cover the entire UHF RFID band, and the volumes are very large. The antennas proposed in [18, 21] have a compact size, whereas the overlapping operating bandwidth does not meet the requirements.

V. CONCLUSION

A novel broadband CPW-fed CPSSA is proposed. The inverted Z-shaped bent feedline and the arc-shaped grounded strip realize impedance matching and CP characteristics, respectively. By widening the width of the vertical tuning stub of the L-shaped grounded strip embedded in the lower-left corner of the square slot, the impedance matching and CP performance can be improved. Finally, a CP reader antenna with broadband characteristic is obtained. The measured 10 dB impedance bandwidth is 64.4% (652-1272 MHz), and the 3 dB axial ratio bandwidth is 32.0% (840-1160 MHz). The operating bandwidth covers the universal UHF RFID band. The overall size of the proposed antenna is $119 \times 119 \times 0.5$ mm³, which has a wider operating bandwidth compared to other broadband antennas with similar dimensions. The measured peak gain is about 4.4 dBi and radiation efficiency is about 90% in the universal UHF RFID band. The proposed antenna has the advantages of simple structure, low cost, compact size, and good bidirectional radiation characteristic in the x-z and y-z planes, making

it more suitable for universal UHF RFID handheld readers applications.

ACKNOWLEDGMENT

This work is supported by Key Project of the National Natural Science Foundation of China under Grant, 62090012, 62031016, 61831017, the Project under Grant 19-163-21-TS-001-062-01, and the Sichuan Provincial Science and Technology Important Projects under Grant 2019YFG0498, 2020YFG0282, 2020YFG0452 and 2020YFG0028.

REFERENCES

- [1] C. Sim and C. Chi, "A slot loaded circularly polarized patch antenna for UHF RFID reader," *IEEE Trans. Antennas Propag.*, vol. 60, no. 10, pp. 4516-4521, Oct. 2012.
- [2] W. Chen and Y. C. Huang, "A novel CP antenna for UHF RFID handheld reader," *IEEE Antennas and Propagation Magazine*, vol. 55, no. 4, pp. 128-137, Aug. 2013.
- [3] C. S. Lee, Y. Fan, and M. Ezzat, "Single-feed circularly polarized microstrip antenna with Bethe holes on the radiating patch," *IEEE Trans. Antennas Propag.*, vol. 68, no. 6, pp. 4935-4938, June 2020.
- [4] M. Shokri, S. Asiaban, and Z. Amiri, "Study, design and fabrication of a CPW fed compact monopole antenna with circular polarization for ultra wide band systems application," *Applied Computational Electromagnetics Society Journal*, vol. 32, no. 9, pp. 749-753, Sep. 2017.
- [5] T. N. Chang and J. M. Lin, "Circularly polarized ring-patch antenna," *IEEE Antennas Wireless Propag. Lett.*, vol. 11, pp. 26-29, Mar. 2012.
- [6] T. Wu, H. Su, L. Gan, H. Chen, J. Huang, and H. Zhang, "A compact and broadband microstrip stacked patch antenna with circular polarization for 2.45-GHz mobile RFID reader," *IEEE Antennas Wireless Propag. Lett.*, vol. 12, pp. 623-626, May 2013.
- [7] J. Z. Huang, P. H. Yang, W. C. Chew, and T. T. Ye, "A novel broadband patch antenna for universal UHF RFID tags," *Microwave Opt. Technol. Lett.*, vol. 52, no. 12, pp. 2653-2657, Dec. 2010.
- [8] X. Chen, G. Fu, S. Gong, Y. Yan, and W. Zhao, "Circularly polarized stacked annular-ring microstrip antenna with integrated feeding network for UHF RFID readers," *IEEE Antennas Wireless Propag. Lett.*, vol. 9, pp. 542-545, June 2010.
- [9] C. Sim, Y. Hsu, and G. Yang, "Slits loaded circularly polarized universal UHF RFID reader antenna," *IEEE Antennas Wireless Propag. Lett.*, vol. 14, pp. 827-830, Nov. 2015.
- [10] X. Liu, Y. Liu, and M. M. Tentzeris, "A novel circularly polarized antenna with coin-shaped patches and a ring-shaped strip for worldwide

- UHF RFID applications,” *IEEE Antennas Wireless Propag. Lett.*, vol. 14, pp. 707-710, Mar. 2015.
- [11] Z. N. Chen, X. Qing, and H. L. Chung, “A universal UHF RFID reader antenna,” *IEEE Trans. Microw. Theory Tech.*, vol. 57, no. 5, pp. 1275-1282, May 2009.
- [12] Y. Pan and Y. Dong, “Circularly polarized stack Yagi RFID reader antenna,” *IEEE Antennas Wireless Propag. Lett.*, vol. 19, no. 7, pp. 1053-1057, July 2020.
- [13] R. Xu, J. Li, J. Yang, K. Wei, and Y. Qi, “A design of u-shaped slot antenna with broadband dual circularly polarized radiation,” *IEEE Trans. Antennas Propag.*, vol. 65, no. 6, pp. 3217-3220, June 2017.
- [14] T. T. Le, H. H. Tran, and H. C. Park, “Simple-structured dual-slot broadband circularly polarized antenna,” *IEEE Antennas Wireless Propag. Lett.*, vol. 17, no. 3, pp. 476-479, Mar. 2018.
- [15] Y. Xu, Z. Wang, and Y. Dong, “Circularly polarized slot antennas with dual-mode elliptic cavity,” *IEEE Antennas Wireless Propag. Lett.*, vol. 19, no. 4, pp. 715-719, Apr. 2020.
- [16] S. Hao, Q. Chen, J. Li, and J. Xie, “A high-gain circularly polarized slotted patch antenna,” *IEEE Antennas Wireless Propag. Lett.*, vol. 19, no. 6, pp. 1022-1026, June 2020.
- [17] Y. F. Lin, Y. C. Kao, S. C. Pan, and H. M. Chen, “Bidirectional radiated circularly polarized annular-ring slot antenna for portable RFID reader,” *Applied Computational Electromagnetics Society Journal*, vol. 25, no.3, pp. 182-189, Mar. 2010.
- [18] C. Raviteja, C. Varadhan, M. Kanagasabai, A. K. Sarma, and S. Velan, “A fractal-based circularly polarized UHF RFID reader antenna,” *IEEE Antennas Wireless Propag. Lett.*, vol. 13, pp. 499-502, Mar. 2014.
- [19] Nasimuddin, Z. N. Chen, and X. Qing, “A compact circularly polarized cross-shaped slotted microstrip antenna,” *IEEE Trans. Antennas Propag.*, vol. 60, no. 3, pp. 1584-1588, Mar. 2012.
- [20] J. Y. Sze, C. I. G. Hsu, M. H. Ho, Y. H. Ou, and M.T. Wu, “Design of circularly polarized annular-ring slot antennas fed by a double-bent microstripline,” *IEEE Trans. Antennas Propag.*, vol. 55, no. 11, pp. 3134-3139, Nov. 2007.
- [21] J. K. Pakkathillam, M. Kanagasabai, and M. G. N. Alsath, “Compact multiservice UHF RFID reader antenna for near-field and far-field operations,” *IEEE Antennas Wireless Propag. Lett.*, vol. 16, pp. 149-152, Feb. 2017.



Rui Ma was born in Ziyang, Sichuan, China, in 1997. She is currently working toward the Master's degree in Information and Communication Engineering at Southwest Jiaotong University (SWJTU), Chengdu, China.

Her main research interests include antenna design and theory, especially in RFID circularly polarized reader antennas.



Quanyuan Feng (M'06–SM'08) received the M.S. degree in Microelectronics and Solid Electronics from the University of Electronic Science and Technology of China, Chengdu, China, in 1991, and the Ph.D. degree in EM Field and Microwave Technology from Southwest Jiaotong University, Chengdu, China, in 2000.

He is the Head of Institute of Microelectronics, Southwest Jiaotong University, Chengdu, China. He has been honored as the “Excellent Expert” and the “Leader of Science and Technology” of Sichuan Province owing to his outstanding contribution. In recent 5 years, more than 500 papers have been published on *IEEE Transactions on Antennas and Propagation*, *IEEE Transactions on Microwave Theory and Techniques*, *IEEE Antennas and Wireless Propagation Letters* etc, among which more than 300 were registered by SCI and EI.

His current research interests include integrated circuits design, RFID technology, embedded system, wireless communications, antennas and propagation, microwave and millimeter wave technology, smart information processing, electromagnetic compatibility, RF/ microwave devices and materials etc.